THE JOURNAL OF PHYSICAL CHEMISTRY C

Article

pubs.acs.org/JPCC

Quantitative Spectra–Structure Relations for Borohydrides

Vincenza D'Anna,*[,†,‡] Latévi Max Lawson Daku,[†] and Hans Hagemann[†]

[†]Département de chimie physique, Sciences II, Université de Genève, 30, Quai Ernest-Ansermet CH-1211 Genève 4, Switzerland

[‡]CNRS, 46 Allee Italie, F-69364 Lyon 07, France

Supporting Information

ABSTRACT: Among the different potential hydrogen storage materials, borohydrides have been largely investigated because of their high gravimetric and volumetric hydrogen content. In the analysis of borohydrides, vibrational spectroscopy plays an important role since it gives information on the local structure of the BH_4^- ion inside the solid. Here the GF method, developed by Wilson, is used in order to determine the local symmetry of BH_4^- in solid borohydrides starting from their vibrational spectra. Two different cases of deformations of BH_4^- are considered. In the first case, the effects of small angular variations on the vibrational spectra of borohydrides will be taken into account; starting from the splitting of the bands corresponding to the deformation modes, the angular deformations will be estimated. In the second one, the BH_4^- under chemical pressure (in different cubic alkali halides) is considered; in this case, the symmetry of the BH_4^- remains T_d, while the bond lengths change according to the pressure experienced. Different practical examples will be illustrated.

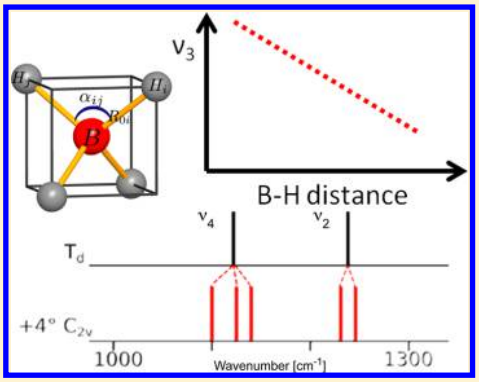

INTRODUCTION

With the perspective to find an alternative to the "oil" economy, the use of hydrogen is quite promising because of its high weight energy content[1] and the negligible environmental impact of its oxidation.[2] However, the problem related to the storage of hydrogen in vehicles is one of the main obstruction to the transition to the "hydrogen economy".[3] In order to overcome this problem, several research projects have been devoted to find materials suitable to store hydrogen at conditions of temperature and pressure practically achievable. All the characteristics of a practical usable hydrogen storage material are summarized in the directives of the U.S. Department of Energy (DOE);[4] presently, there are no materials that fulfill the DOE requirements.[1,5,6] Among the potential hydrogen storage materials, borohydrides have been largely investigated because of their high gravimetric and volumetric hydrogen content (see, for example, ref 7 and references therein).

Spectroscopic techniques like NMR and vibrational spectroscopy can contribute to describe the local structure in a given system. This is particularly useful in the case of hydrogen-containing compounds, where powder X-ray diffraction is inherently not the best method to localize accurately the hydrogen atoms.

Group theory predicts the splittings of vibrational bands expected upon lowering the symmetry of a tetrahedral ion into a given crystal. However, the magnitude of these splittings is not predicted.

In this work, we apply the well-known GF method[8] for vibrational spectroscopy to study the effect of small angular deformations on the tetrahedral BH_4^- ion. In the second part, we study the effect of bond length change on the vibrational frequencies in tetrahedral symmetry. Within the GF approach, the frequencies are calculated from the solution of the secular equation relating the force constant matrix ($\mathbf{F}$) and the matrix containing information about the geometry and the atomic masses of the system ($\mathbf{G}$):

$$|\mathbf{GF} - \mathbf{I}\lambda| = 0 \quad (1)$$

where $\mathbf{I}$ is the identity matrix and λ is related with the vibrational frequencies (ν):

$$\lambda = 4\pi^2\nu^2 \quad (2)$$

The initial force field used results from a DFT calculation on an individual BH_4^- ion, while historically the force field was often parametrized from experimental data. Different theoretical calculations lead obviously to different force matrices and different vibrational frequencies. However, as will be shown in this paper, the magnitudes of the splittings of the degenerate modes upon deformations are very similar. A further matter of concern is the effect of anharmonicity and Fermi resonances. In a previous paper,[9] we studied in detail the Fermi resonances observed in the cubic alkali borohydrides and deuterides. Significant differences between harmonic and anharmonic frequencies were observed. In order to take indirect account of these effects, the stretching force constants were adjusted using experimental stretching frequencies to correlate the stretching frequencies with B–H bond length.

In the first part of this study, the force field is kept fixed, and only the $\mathbf{G}$-matrix is changed in order to simulate different

Received: June 25, 2015
Revised: August 31, 2015
Published: September 1, 2015

DOI: 10.1021/acs.jpcc.5b06045
J. Phys. Chem. C 2015, 119, 21868–21874

angular variations and to calculate the resulting vibrational frequencies. These calculated results are compared with the experimental vibrational spectra of $LiBH_4$ and $NaBH_4$. In the second part, we first show by comparison with experimental data that only the diagonal B−H stretching force constants change significantly with the bond length. We then will study the evolution of the experimental vibrational spectra of the tetrahedral BH_4^- ion in many different cubic crystalline environments.

The approach presented here is general and can be easily applied to other tetrahedral systems such as AlH_4^- or extended to other systems with different symmetry (XY_6, $X_{12}Y_{12}$, etc.)

BACKGROUND: THE GF METHOD FOR TETRAHEDRAL SYSTEM

The GF method[8] is a classical mechanics[10] method, which allows the description of the small-amplitude vibrations of a molecule about its equilibrium geometry in terms of its normal coordinates. Before going in the detailed derivation of the method for the title molecule, we give a brief overview of the method, while putting the emphasis on the physical meaning of the **G** and **F** matrices.

For a molecule of N atoms with n internal degrees of freedom described by the internal coordinates $\mathbf{R} = (R_i)_{i=1,...,n}$, the Lagragian reads:

$$\mathcal{L} = \underbrace{\frac{1}{2}\sum_{ik} a_{ik}(\mathbf{R})\dot{R}_i\dot{R}_k}_{T(\mathbf{R},\dot{\mathbf{R}})} - V(\mathbf{R}) \tag{3}$$

where $\dot{X}$ denotes the time derivative of X; $T(\mathbf{R}, \dot{R})$ is the kinetic energy of the system, without the contributions from the rotational and the translational degrees of freedom; and $V(\mathbf{R})$ is the potential energy. The coefficients $a_{ik}(\mathbf{R})$ are given by

$$a_{ik}(\mathbf{R}) = \sum_{j=1}^{N} m_j \frac{\partial \mathbf{z}_j}{\partial R_i}\cdot\frac{\partial \mathbf{z}_j}{\partial R_k} \tag{4}$$

where m_j is the mass of the jth atom; $\mathbf{z}_j$ its Cartesian coordinates expressed in terms of the generalized coordinates: $\mathbf{z}_j = \mathbf{z}_j(R_1,...,R_n) = \mathbf{z}_j(\mathbf{R})$; and where " · " denotes the scalar product.

Taking the equilibrium geometry as the origin O and setting $V(O) = 0$, the second-order Taylor series expansions about O of the kinetics and the potential energy potential energies are given by

$$T(\mathbf{R}, \dot{R}) = \frac{1}{2}\sum_{ik} a_{ik}(O)\dot{R}_i\dot{R}_k \tag{5}$$

$$V(\mathbf{R}) = \frac{1}{2}\sum_{ik} F_{ik}R_iR_k \tag{6}$$

From the Lagrange equations of motion

$$\frac{\mathrm{d}}{\mathrm{d}t}\left(\frac{\partial \mathcal{L}}{\partial \dot{R}_i}\right) - \frac{\partial \mathcal{L}}{\partial R_i} = 0 \tag{7}$$

we obtain the set of n equations

$$\sum_k a_{ik}(O)\ddot{R}_k = \sum_{ik} F_{ik}R_k \tag{8}$$

which can be put in the matricial form

$$\mathbf{A}\ddot{R} = \mathbf{FR} \tag{9}$$

with $\mathbf{A} = (a_{ik}(O))_{i,k=1...,n}$ a symmetric positive-definite matrix ($T > 0$) and $\mathbf{F} = (F_{ik})_{i,k=1\cdots,n}$. Putting $\mathbf{G} = \mathbf{A}^{-1}$, the above equation can also be written

$$\ddot{R} = \mathbf{GFR} \tag{10}$$

whose solution relies on the determination of the eigenvalues of the **GF** matrix:

$$\mathbf{GFP} = \mathbf{P\Lambda} \tag{11}$$

P is the matrix whose columns are the eigenvectors of **GF**, and $\mathbf{\Lambda} = \mathbf{diag}(\lambda_i)_{i=1,...,n}$ the diagonal matrix made of its eigenvalues λ_i. We thus see that, for small-amplitudes changes in the internal coordinates about the equilibrium molecular geometry, $\mathbf{G}^{-1}$ and **F** help express the kinetic energy and the harmonic potential energy of the internal coordinates, respectively. Setting $\mathbf{Q} = \mathbf{P}^{-1}\mathbf{R}$, the eigenvalue problem reads

$$\ddot{Q} = \mathbf{\Lambda Q} \tag{12}$$

The columns of **Q** are the so-called normal coordinates.

The G Matrix. According to Wilson,[8] the first step for the construction of the **G** matrix consists in the determination of a relation between the internal and the Cartesian coordinates; the choice of the internal coordinates is convenient since the variations of the internal coordinates correspond to the stretching and bending modes.

The matricial expression of the relation between internal and Cartesian coordinates is given in eq 13:

$$\mathbf{R} = \mathbf{Bx} \tag{13}$$

where **R** and **x** are the internal and Cartesian coordinates vectors, respectively, and **B** is the geometry transformation matrix. The linear form of the eq 13 is

$$R_k = \sum_{i=1}^{3N} B_{ki}x_i, \qquad k = 1, 2, ..., 3N - 6 \tag{14}$$

where N is the number of atoms.

From the **B** matrix, it is possible to obtain the **G** matrix, since it is defined as the row by row product of the **B** matrix weighed by the atomic masses:[8]

$$\mathbf{G} = \mathbf{BM}^{-1}\mathbf{B} \tag{15}$$

Each element of the **G** matrix is, then, expressed as

$$G_{kl} = \sum_{i=1}^{3N} \frac{B_{ki}B_{li}}{m_i}, \qquad k, l = 1, 2, ..., 3N - 6 \tag{16}$$

For $1 \le i \le 3$, m_i refers to the first atom, for $4 \le i \le 6$, m_i refers to the second one, *et cetera*.

In order to apply the procedure of the construction of the **G** matrix to a tetrahedral system, the internal and Cartesian coordinates of the equilibrium positions and of the displacements from the equilibrium should be defined; henceforth, everything will be referred to the BH_4^- group.

The Cartesian coordinates of the equilibrium positions and of the displacements, with respect to an arbitrary reference system, are summarized in Table 1, while the internal coordinates (10 in total, including 4 bond lengths and 6 angles) at equilibrium positions are shown in Figure 1. Accordingly, Δr_i and $\Delta\alpha_{ij}$ are the displacement from equilibrium position expressed in terms of internal coordinates and they correspond to the stretching and the bending modes,

DOI: 10.1021/acs.jpcc.5b06045
J. Phys. Chem. C 2015, 119, 21868−21874

Table 1. Equilibrium Positions and Displacements from Equilibrium Expressed in Cartesian Coordinates for the BH_4^- Group[a]

atom	coordinates	displacement
B	X_0, Y_0, Z_0	x_0, y_0, z_0
H_1	X_1, Y_1, Z_1	x_1, y_1, z_1
H_2	X_2, Y_2, Z_2	x_2, y_2, z_2
H_3	X_3, Y_3, Z_3	x_3, y_3, z_3
H_4	X_4, Y_4, Z_4	x_4, y_4, z_4

[a]An arbitrary system of reference is considered.

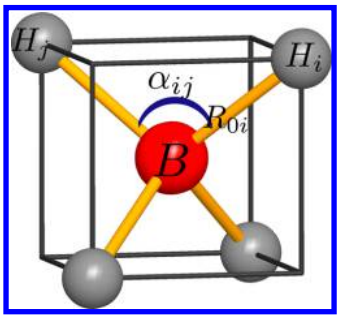

Figure 1. Internal coordinates chosen to express the equilibrium position for BH_4^-.

respectively. It should be noted that, for a nonlinear molecule consisting of five atoms, the degrees of freedom are nine; in this case 10 coordinates are considered, treating, then, the redundancy in explicit way.

The expressions of Δr_i and $\Delta\alpha_{ij}$ in terms of x_i, y_i, z_i are given in eqs 17 and 18, respectively. All the mathematical procedures are shown in the Supporting Information.

$$\Delta r_i = \left\|\overrightarrow{BH_i}\right\| - \left\|\overrightarrow{BH_{i_{eq}}}\right\|$$
$$= R_{0i} + \frac{X_{0i}}{R_{0i}}x_i + \frac{Y_{0i}}{R_{0i}}y_i + \frac{Z_{0i}}{R_{0i}}z_i - \frac{X_{0i}}{R_{0i}}x_0 - \frac{Y_{0i}}{R_{0i}}y_0 - \frac{Z_{0i}}{R_{0i}}z_0 - R_{0i}$$
$$= \frac{X_{0i}}{R_{0i}}x_i + \frac{Y_{0i}}{R_{0i}}y_i + \frac{Z_{0i}}{R_{0i}}z_i - \frac{X_{0i}}{R_{0i}}x_0 - \frac{Y_{0i}}{R_{0i}}y_0 - \frac{Z_{0i}}{R_{0i}}z_0 \quad (17)$$

$$\Delta\alpha_{ij} = x_0\frac{X_{0i}(R_{0i}R_{0j} - {R_{0j}}^2\cos\alpha_{ij}) + X_{0j}(R_{0i}R_{0j} - {R_{0i}}^2\cos\alpha_{ij})}{{R_{0i}}^2{R_{0j}}^2\sin\alpha_{ij}}$$
$$+ y_0\frac{Y_{0i}(R_{0i}R_{0j} - {R_{0j}}^2\cos\alpha_{ij}) + Y_{0j}(R_{0i}R_{0j} - {R_{0i}}^2\cos\alpha_{ij})}{{R_{0i}}^2{R_{0j}}^2\sin\alpha_{ij}}$$
$$+ z_0\frac{Z_{0i}(R_{0i}R_{0j} - {R_{0j}}^2\cos\alpha_{ij}) + Z_{0j}(R_{0i}R_{0j} - {R_{0i}}^2\cos\alpha_{ij})}{{R_{0i}}^2{R_{0j}}^2\sin\alpha_{ij}}$$
$$+ x_i\frac{X_{0i}R_{0j}\cos\alpha_{ij} - X_{0j}R_{0i}}{{R_{0i}}^2R_{0j}\sin\alpha_{ij}} + y_i\frac{Y_{0i}R_{0j}\cos\alpha_{ij} - Y_{0j}R_{0i}}{{R_{0i}}^2R_{0j}\sin\alpha_{ij}}$$
$$+ z_i\frac{Z_{0i}R_{0j}\cos\alpha_{ij} - Z_{0j}R_{0i}}{{R_{0i}}^2R_{0j}\sin\alpha_{ij}} + x_j\frac{X_{0j}R_{0i}\cos\alpha_{ij} - X_{0i}R_{0j}}{{R_{0j}}^2R_{0i}\sin\alpha_{ij}}$$
$$+ y_j\frac{Y_{0j}R_{0i}\cos\alpha_{ij} - Y_{0i}R_{0j}}{{R_{0j}}^2R_{0i}\sin\alpha_{ij}} + z_j\frac{Z_{0j}R_{0i}\cos\alpha_{ij} - Z_{0i}R_{0j}}{{R_{0j}}^2R_{0i}\sin\alpha_{ij}} \quad (18)$$

The expressions of Δr_i and $\Delta\alpha_{ij}$ are the basis for the construction of the **B** matrix. In this case, the size of the **B** matrix is 10 × 15, since there are 10 internal and 15 Cartesian coordinates. Each row of the **B** matrix contains the expression of the displacement from an equilibrium position in internal coordinates as a function of the Cartesian ones. In particular, the first four rows of the **B** matrix are inherent to the B−H bond lengths, while the other six ones refer to the $H\hat{B}H$ angles. The complete expression of the **B** matrix is shown in the Supporting Information.

A second force field was also obtained from coupled-cluster calculations performed at the CCSD(T)/aug-cc-pVTZ level. The calculated frequencies are different by at most 50 cm^{-1}, however the splittings of the ν_3 and ν_4 modes upon an angular deformation of 4° are very similar (see Supporting Information).

Starting from the **B** matrix, the **G** matrix was constructed according to eq 15. The **G** matrix is a symmetric matrix with 10 × 10 size; each index with value less or equal than 4 is relative to a bond length, otherwise it refers to an angle. Accordingly, in the **G** matrix three different blocks can be identified: stretch−stretch ($1 \le i,j \le 4$), bend−bend ($i,j > 4$) and stretch−bend ($i \le 4, j > 4$ or $j \le 4, i > 4$). Inside each block, different kinds of elements can be identified. In particular, inside the stretch−stretch block, there are the diagonal and the out of diagonal elements; a diagonal element is inherent to the variation of only one bond length, while an out of diagonal element takes into account two bond lengths. In the bend−bend block there are three kinds of elements: the diagonal ones, relative to the variation of one angle, the elements that consider pairs of angles sharing one terminal atom and elements inherent to pairs of angles that do not share any terminal atoms. Finally, in the stretch−bend block, there are two different kinds of elements describing the case in which the terminal atom of the bond is involved in the angle and the case where the terminal atom of the bond is not part of the angle. The elements of the **G** matrix were implemented in a SCILAB[11] program where the values of atomic masses, bond lengths, and bond angles were the input values. Examples of the different elements of the **G** matrix and their general expressions are shown in the Supporting Information.

The F Matrix. The force constant matrix was obtained from a calculation on the isolated BH_4^- group within Density Functional Theory (DFT). The calculation was performed using Gaussian 09[12] package, the B3LYP[13,14] hybrid functional and the 6-31g(d,p) basis set of valence double-ζ polarized quality.[15,16] In this calculation, the symmetry of the BH_4^- was kept T_d. The input file was prepared in such a way that the **F** matrix was expressed in the same internal coordinates as the **G** matrix. Consequently, also the **F** matrix is a 10 × 10 symmetric matrix, and shows the stretch−stretch, bend−bend and stretch−bend blocks. The **F** obtained from Gaussian calculations is shown in the Supporting Information.

In the first part of this study, where the frequencies dependence on the small angular variations of BH_4^- are taken into account, the **F** matrix will be considered constant. In fact, as long as no bond length changes are considered, this approximation is reasonable.[17,18] In the second part of this work, where the effect on the vibrational frequencies of the B−H bond length variation is analyzed, the **F** matrix cannot be considered constant anymore. However, at this stage, only the stretch−stretch part is changed, and the relation between the

DOI: 10.1021/acs.jpcc.5b06045
J. Phys. Chem. C 2015, 119, 21868−21874

Table 2. Correlation Table of T_d Group

	T_d	D_{2d}	C_{3v}	S_4	D_2	C_{2v}	C_3	C_2	C_s
ν_1	a_1	a_1	a_1	a	a	a_1	a	a	a'
	a_2	b_1	a_2	b	a	a_2	a	a	a''
ν_2	e	$a_1 + b_1$	e	$a + b$	$2a$	$a_1 + a_2$	e	$2a$	$a' + 2a''$
	t_1	$a_2 + e$	$a_2 + e$	$a + e$	$b_1 + b_2 + b_3$	$a_2 + b_1 + b_2$	$a + e$	$a + 2b$	$a' + 2a''$
ν_3, ν_4	t_2	$b_2 + e$	$a_1 + e$	$b + e$	$b_1 + b_2 + b_3$	$a_1 + b_1 + b_2$	$a + e$	$a + 2b$	$2a' + a'$

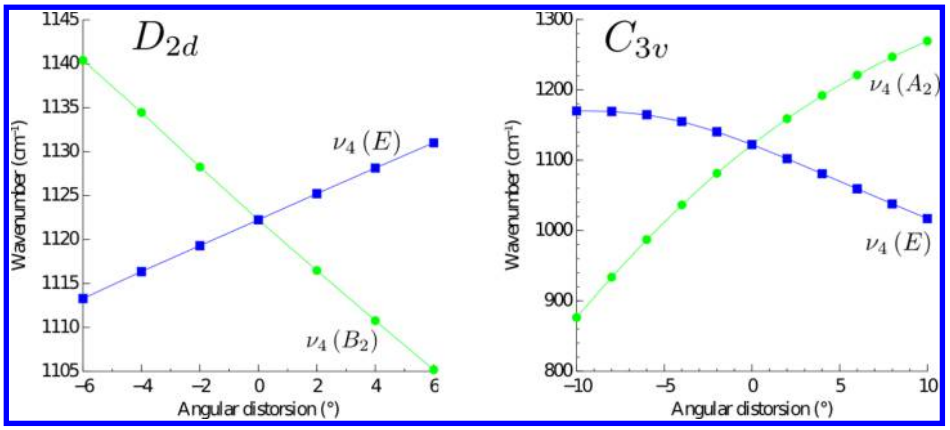

Figure 2. Angular dependence of the splitting of the ν_4 mode in D_{2d} (left) and C_{3v} (right) symmetry.

stretch−stretch force constant elements and the bond length will be discussed.

RESULTS AND DISCUSSION

Small Angular Variations. In this section the effect of the lowering of the BH_4^- symmetry on its vibrational spectrum is analyzed. In particular the symmetry was lowered from T_d to D_{2d}, C_{3v}, and C_{2v} through small angular variations, as shown in eqs 19, 20 and 21, respectively; the nomenclature of the angles is given according to Table 1.

$$\alpha_{12} = \alpha_{34} \text{ and } \alpha_{13} = \alpha_{14} = \alpha_{23} = \alpha_{24} \quad (19)$$

$$\alpha_{12} = \alpha_{13} = \alpha_{14} \text{ and } \alpha_{23} = \alpha_{24} = \alpha_{34} \quad (20)$$

$$\alpha_{13} = \alpha_{14} = \alpha_{23} = \alpha_{24} \text{ and } \alpha_{34} = 109.471 \quad (21)$$

Group theory predicts the observation of splitting of degenerate vibrational modes with decreasing symmetry. Correlation table of the T_d group (see Table 2) indicates the irreducible representations obtained in subgroups of the T_d group.

The GF method allows to quantify the extent of the splitting as a function of the angular deformations according to the eqs 19, 20, and 21. Considering the triply degenerate deformation mode ν_4, it appears that a trigonal deformation leading to C_{3v} results in a huge splitting compared to the one obtained in the deformation leading to D_{2d}. This behavior is shown in Figure 2.

In the high pressure experiments on $RbBH_4$[19] it was noted the formation of a tetragonal phase above 3 GPa; in this phase the site symmetry of the BH_4^- ion is D_{2d}. At 4.8 GPa, the Raman spectra show a splitting of 10 cm^{-1} of the ν_4 bands. According to Figure 2, this splitting corresponds to an angular distortion of ca. 2°.

$NaBH_4$ becomes tetragonal at low temperatures. The Raman spectrum at 80 K in Figure 3 shows a splitting of only 5 cm^{-1}, corresponding to only 1° deformation.

In the high temperature phase of $LiBH_4$ ($P6_3mc$), the BH_4^- group is located on a site with C_{3v} symmetry.[20] The experimental IR spectrum, shown in Figure 4, reveals a splitting

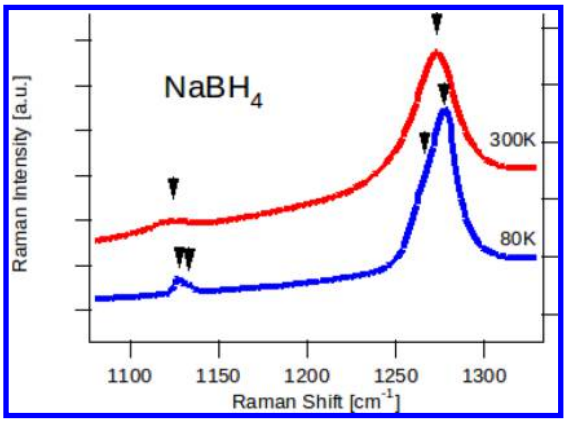

Figure 3. Raman spectra of $NaBH_4$ at ca. 80 and 300 K. (The spectra are vertically shifted for clarity). Raman spectra were obtained with a Kaiser Optical Holospec Raman monochromator equipped with a liquid nitrogen-cooled CCD camera. Spectra were obtained in a home-built liquid nitrogen coldfinger Dewar using 50 mW laser excitation at 488 nm.

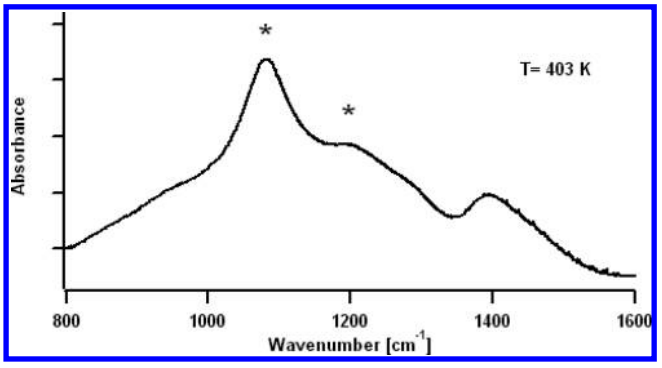

Figure 4. IR spectrum of $LiBH_4$ measured at 403 K. The splitting discussed in the main text is between the two peaks indicated by an asterisk.

DOI: 10.1021/acs.jpcc.5b06045
J. Phys. Chem. C 2015, 119, 21868−21874

of ca. 110 cm^{-1} of the ν_4 mode, corresponding to an estimated angular deformation of 3.7° according to Figure 2. Neutron diffraction experiments[20] on $LiBD_4$ indicated a distortion of 3°, but the very large thermal ellipsoids for the hydrogen (deuterium) atoms in the crystal makes the experimental value not very accurate.

Bond Length Variation. Once the bond length dependence of the vibrational frequencies is considered, the **F** matrix cannot be kept constant anymore and its dependence on the B−H distances should be taken into account.[17,18] It has been shown previously[21,22] that it is possible to apply Badger's rule[17,18] to correlate the B−D stretching frequencies with the experimental B−D bond lengths obtained from neutron diffraction for the cubic alkali borohydrides.

Using the experimental vibrational frequencies and bond lengths for the cubic alkali borohydrides,[21,22] the elements of the stretch−stretch block of the **F** matrix were adjusted to reproduce the experimental values of the stretching frequencies. The results, collected in Table 3, show that the out-of-diagonal

Table 3. Diagonal (F_{ii}, $i \leq 4$) and Out-of-Diagonal (F_{ij}, $i,j \leq 4$) Force Constant Values for MBH_4 (M = Na, K, Rb, Cs) Series[a]

compound	F_{ii}	F_{ij}	B−H length	GF frequencies	exp frequencies
$NaBH_4$	0.192	0.006	1.178(2)	2341 (ν_1)	2340 (ν_1)
				2325 (ν_3)	2321 (ν_3)
KBH_4	0.187	0.006	1.196(3)	2315 (ν_1)	2312 (ν_1)
				2290 (ν_3)	2288 (ν_3)
$RbBH_4$	0.184	0.006	1.206(2)	2299 (ν_1)	2300 (ν_1)
				2273 (ν_3)	2273 (ν_3)
$CsBH_4$	0.181	0.006	1.217(3)	2285 (ν_1)	2287 (ν_1)
				2255 (ν_3)	2255 (ν_3)

[a]The values are expressed in internal units (hartrees−bohrs−radians). The experimental B-D distance (Å)[21,22] and the experimental[21−23] and GF calculated frequencies (cm^{-1}) are also shown.

elements remain constant, F_{ij} = 0.006 electron mass/(atomic unit of time)^2, while the diagonal force constants appear to change linearly with the bond length, following eq 22:

$$F(ii) = 0.46542 - 0.12351 \cdot R_{0i} i \leq 4 \quad (22)$$

The GF calculated bending modes (ν_2 and ν_4) were compared with the ones calculated by using the unmodified Gaussian force matrix, in order to quantify the dependence of the bending modes from the stretch−stretch part of the **F** matrix. The two sets of values were found to be almost identical, and this means that the different blocks of the matrices are practically independent. The GF calculated bending modes were also compared with the experimental data (see Table 4). Table 4 shows that, for all the systems, the GF calculated bending modes are overestimated by about the same amount.

This modified **F** matrix was applied to the study of BH_4^- diluted in different alkali halides ($MX:BH_4$ with M = Na, K, Rb, Cs and X = Cl, Br, I). Figure S1 of the Supporting Information shows the stretching and bending IR frequencies plotted vs the cubic lattice parameter *a*. The scatter of the data suggests that the tetrahedral BH_4^- ions experience different local (chemical) pressures due to the different ionic sizes. This local pressure translates then into the B−H bond length change. Using the experimentally observed frequencies,[24−27] the corresponding bond length were estimated in the following way: the value of

Table 4. GF Calculated and Experimental[21−23] Bending Modes (ν_2 and ν_4) and Difference between Calculated and Experimental Modes ($\Delta\nu_i = \nu_i^{GF} - \nu_i^{exp}$)[a]

	ν_2		ν_4			
MBH_4	expt	calcd	expt	calcd	$\Delta\nu_2$	$\Delta\nu_4$
$NaBH_4$	1274	1312	1124	1188	38	64
KBH_4	1246	1285	1119	1164	39	45
$RbBH_4$	1234	1272	1112	1152	38	40
$CsBH_4$	1220	1263	1103	1144	43	41

[a]All the values are expressed in cm^{-1}.

the bond length (in eq 22) was varied until the GF calculated frequency matched the experimental frequency of the ν_3 stretching mode. The results are summarized in Figure 5

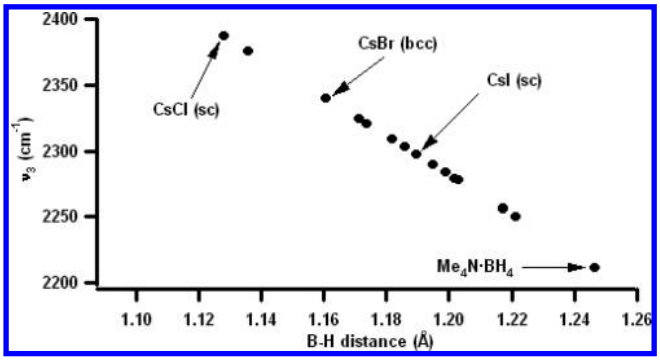

Figure 5. Stretching ν_3 vibrational modes (cm^{-1}) versus GF calculated B−H distances (Å) for the BH_4^- ion diluted in alkali halides and for $Me_4N{\cdot}BH_4$. Experimental data from references.[24−27]

Figure 6 compares the calculated and observed ν_4 deformation frequencies for different B−H bond lengths. For

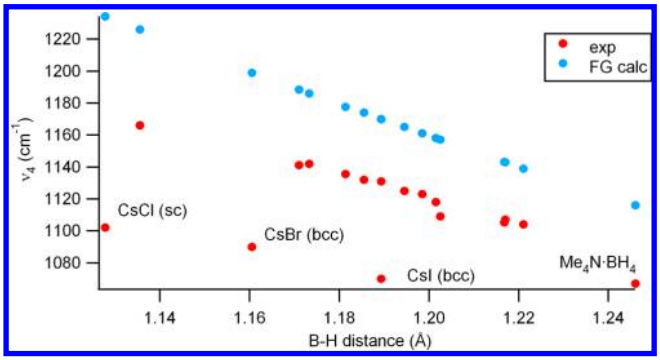

Figure 6. Experimental (red dots) and GF calculated (blue dots) ν_4 bending vibrational modes (cm^{-1}) versus GF calculated B−H distances (Å) for the BH_4^- ion diluted in alkali halides. Experimental data were from the literature.[24−27] For $Me_4N{\cdot}BH_4$, the B−H distance calculated with GF method is used in both curves, experimental and GF calculated.

most of the data, there is a systematic shift of about 40 cm^{-1}, as already noted above (see Table 4).

However, the data points for BH_4^- diluted in cesium halides do not follow this trend. These host crystals have simple cubic (sc) or body centered cubic (bcc) structures, in contrast to all the others which have face centered cubic structures (fcc). It is interesting to note that these three data points are also aligned. In the fcc structure, the BH_4^- ion is surrounded by an

DOI: 10.1021/acs.jpcc.5b06045
J. Phys. Chem. C 2015, 119, 21868−21874

octahedron of six cations, while in the sc and bcc structure, it is surrounded by a cube of eight cations. The different behavior in Figure 6 suggests that one has also to consider the cation coordination which influences the values of the bending frequencies. These results can also be applied to high pressure studies of the alkali borohydrides in their cubic phases. The slope of Figure 5 indicates that the bond length changes by 0.01 Å for a frequency shift of 15 cm^{-1} for ν_3 and 13 cm^{-1} for the Raman active ν_1. In the case of $NaBH_4$[28] a pressure shift of ca. 25 cm^{-1}/GPa was observed in the $Fm\bar{3}m$ phase up to 2 GPa, corresponding to an estimated shortening of the B−H bond of about 0.02 Å.

CONCLUSIONS

We have applied the GF method to calculate the amplitude of angular deformations observed for alkali borohydrides and compared the results with observed experimental spectra. The force field for this calculation was first obtained from DFT calculations for an individual ion. The theoretical level of the calculations does not influence significantly the magnitudes of the splittings upon angular deformations. Our observations also show that the bending mode frequencies are influenced by the coordination of cations around the BH_4^- ion. This aspect requires further investigations.

Using the published crystal structure data for MBH_4 (M = Na, K, Rb, Cs) and the vibrational spectra of these compounds, we found that an empirical linear relation describes the change of the diagonal B−H stretching force constant with change of the bond length. The application of this relation to a set of experimental data for borohydrides in cubic crystals shows that the B−H bond length varies by more than 0.1 Å in the series of compounds studied. Pressure dependent results for $NaBH_4$ are also discussed. It is important to stress that for the two parts of this study, we have either kept the B−H bond length fixed (for the angular deformations) or constrained the geometry to tetrahedral symmetry. Deformations combining both bond length changes and angular deformations will require further investigations to identify the dominating contributions in the **F** matrix. The approach illustrated in the present work is general and can be applied to other molecules. An interesting study in the field of boron hydrogen compounds could by the study of different deformations of icosahedron $B_{12}H_{12}^{2-}$.

ASSOCIATED CONTENT

Supporting Information

The Supporting Information is available free of charge on the ACS Publications website at DOI: 10.1021/acs.jpcc.5b06045.

Detailed mathematical description for the tetrahedral molecule, as well as the results from the coupled-cluster calculations, and the plot for BH_4^- in cubic crystals of the stretching and bending IR frequencies as functions of the lattice parameter (PDF)

AUTHOR INFORMATION

Corresponding Author

*(V.D.) E-mail: Vincenza.Danna@ens-lyon.fr.

Notes

The authors declare no competing financial interest.

ACKNOWLEDGMENTS

This work was supported by the Swiss national Science Foundation.

REFERENCES

(1) Suh, M. P.; Park, H. J.; Prasad, T. K.; Lim, D.-W. Hydrogen Storage in Metal-Organic Frameworks. *Chem. Rev.* **2012**, *112*, 782−835.
(2) Corbo, P.; Migliardini, F.; Veneri, O. *Hydrogen Fuel Cells for Road Vehicles*; Green Energy and Technology; Springer: Berlin, 2011.
(3) Eberle, U.; Felderhoff, M.; Schüth, F. Chemical and Physical Solutions for Hydrogen Storage. *Angew. Chem., Int. Ed.* **2009**, *48*, 6608−6630.
(4) http://www1.eere.energy.gov/hydrogenandfuelcells/storage/current_technology.html (last visited: 2013-14-02).
(5) Yang, J.; Sudik, A.; Wolverton, C.; Siegel, D. J. High capacity hydrogen storage materials: attributes for automotive applications and techniques for materials discovery. *Chem. Soc. Rev.* **2010**, *39*, 656−675.
(6) McWhorter, S.; O'Malley, K.; Adams, J.; Ordaz, G.; Randolph, K.; Stetson, N. T. Moderate Temperature Dense Phase Hydrogen Storage Materials within the US Department of Energy (DOE) H_2 Storage Program: Trends toward Future Development. *Crystals* **2012**, *2*, 413−445.
(7) Severa, G.; Hagemann, H.; Longhini, M.; Kaminski, J. K.; Wesolowski, T. A.; Jensen, C. M. Thermal Desorption, Vibrational Spectroscopic, and DFT Computational Studies of the Complex Manganese Borohydrides $Mn(BH_4)_2$ and $[Mn(BH_4)_4]^{2-}$. *J. Phys. Chem. C* **2010**, *114*, 15516−15521.
(8) Wilson, E. B. A., Jr. Method of Obtaining the Expanded Secular Equation for the Vibration Frequencies of a Molecule. *J. Chem. Phys.* **1939**, *7*, 1047−1052.
(9) Carbonnière, P.; Hagemann, H. Fermi Resonances of Borohydrides in a Crystalline Environment of Alkali Metals. *J. Phys. Chem. A* **2006**, *110*, 9927−9933.
(10) Landau, L. D.; Lifshitz, E. M. *Mécanique*, quatrième édition ed.; Physique Théorique; Mir: Moscow, 1982; Vol. *1*.
(11) Scilab Enterprises *Scilab: Free and Open Source software for numerical computation*; Scilab Enterprises: Orsay, France, 2012.
(12) Frisch, M. J. et al. Gaussian 09 Revision A.1. Gaussian Inc.: Wallingford CT, 2009.
(13) Becke, A. D. Density-functional thermochemistry. III. The role of the exact exchange. *J. Chem. Phys.* **1993**, *98*, 5648−5652.
(14) Stephens, P. J.; Devlin, F. J.; Chabalowski, C. F.; Frisch, M. J. *Ab initio* calculations of vibrational absorption and circular dichroism spectra using density functional theory force fields. *J. Phys. Chem.* **1994**, *98*, 11623−11627.
(15) Petersson, G. A.; Bennett, A.; Tensfeldt, T. G.; Al-Laham, M. A.; Shirley, W. A.; Mantzaris, J. A complete basis set model chemistry. I. The total energies of closed-shell atoms and hydrides of the first-row atoms. *J. Chem. Phys.* **1988**, *89*, 2193−2218.
(16) Petersson, G. A.; Al-Laham, M. A. A complete basis set model chemistry. II. Open-shell systems and the total energies of the first-row atoms. *J. Chem. Phys.* **1991**, *94*, 6081−6090.
(17) Badger, R. M. A. Relation Between Internuclear Distances and Bond Force Constants. *J. Chem. Phys.* **1934**, *2*, 128−131.
(18) Badger, R. M. The Relation Between the Internuclear Distances and Force Constants of Molecules and Its Application to Polyatomic Molecules. *J. Chem. Phys.* **1935**, *3*, 710−714.
(19) Filinchuk, Y.; Talyzin, A. V.; Hagemann, H.; Dmitriev, V.; Chernyshov, D.; Sundqvist, B. Cation Size and Anion Anisotropy in Structural Chemistry of Metal Borohydrides. The Peculiar Pressure Evolution of $RbBH_4$. *Inorg. Chem.* **2010**, *49*, 5285−5292.
(20) Hartman, M. R.; Rush, J. J.; Udovic, T. J.; Bowman, R. C., Jr.; Hwang, S.-J. Strucutre and vibrational dynamics of isotopically labeled lithium borohydride using neutron diffraction and spectroscopy. *J. Solid State Chem.* **2007**, *180*, 1298−1305.
(21) Renaudin, G.; Gomes, S.; Hagemann, H.; Keller, H.; Yvon, K. Structural and spectroscopic studies on the alkali borohydrides MBH_4 (M = Na, K, Rb, Cs). *J. Alloys Compd.* **2004**, *375*, 98−106.
(22) D'Anna, V.; Spyratou, A.; Sharma, M.; Hagemann, H. Spectrochim. Acta. *Spectrochim. Acta, Part A* **2014**, *128*, 902−906.
(23) Fischer, P.; Züttel, A. Order-Disorder Phase Transition in $NaBD_4$. *Mater. Sci. Forum* **2004**, *443-444*, 287−290.

DOI: 10.1021/acs.jpcc.5b06045
J. Phys. Chem. C 2015, 119, 21868−21874

(24) Ketelaar, J. A. A.; Schutte, C. J. H. The borohydride ion (BH_4^-) in a face-centred cubic alkali-halide lattice. *Spectrochim. Acta* **1961**, *17*, 1240−1243.
(25) Coker, E. H.; Hofer, D. E. Infrared Spectra of Borohydride Ions in Alkali Halide Single Crystals. *J. Chem. Phys.* **1968**, *48*, 2713−2719.
(26) Coker, E. H.; Hofer, D. E. Infrared Spectra of the d_n-Borohydride Ions. *J. Chem. Phys.* **1970**, *53*, 1652−1656.
(27) Schutte, W. C.; Coker, H. Infrared spectra of CsCl:BH_4^- solid solutions. *J. Chem. Phys.* **1974**, *61*, 2808−2809.
(28) Moysés Araújo, C.; Ahuja, R.; Talyzin, A. V.; Sundqvist, B. Pressure-induced structural phase transition in $NaBH_4$. *Phys. Rev. B: Condens. Matter Mater. Phys.* **2005**, *72*, 054125.

DOI: 10.1021/acs.jpcc.5b06045
J. Phys. Chem. C 2015, 119, 21868−21874